6.3 NUMERICAL SIMULATIONS OF THE OROGRAPHIC PRECIPITATION AND MESOSCALE ENVIRONMENTS ASSOCIATED WITH MAP IOP-8

Yuh-Lang Lin, Shu-Yun Chen and Sen Chiao
Department of Marine, Earth, and Atmospheric Sciences,
North Carolina State University, Raleigh, North Carolina, USA

1. Introduction

Both the Swiss Model and the Mesoscale Compressible Community (MC2) model overpredicted rainfall for MAP-IOP-8 starting 99/10/21/00Z over the Lago Maggiore Targeted Area (LMTA) (Bousquet and Smull 2003). In addition, the major rainfall area was displaced over the Po Valley, which is far upstream of the southern Alpine slopes (Houze et al. 2000; Bousquet and Smull 2003).

Based on Doppler radar observations, Bousquet and Smull (2003) documented that during IOP-8 the southerly low-level winds ahead of the eastward propagating deep baroclinic trough was blocked by the Alps far upstream, which reduced the transport of warm and moist airflow from the ocean. In addition, they proposed that the widespread stratiform rainfall has some "orographic" effects in the sense that its development was closely tied to blocked easterly-component, stable flow alongside the Alps at lower levels. A recent study of Rotunno and Ferrati (2003) also suggested that low-level convergence over the western Po valley might be enhanced by the deflection of subsaturated air (subsequently cooled and stabilized through evaporation of precipitation) blocked by the Alps. The PSU/NCAR MM5 model was used to simulate the MAP IOP-8 orographic rainfall event. Three nested domains are adopted to simulate the synoptic and mesoscale environments. Domains 1, 2 and 3 use 45, 15 and 5 km grid resolution, respectively. The 45-km resolution simulation is initialized at 12Z 19 October 1999 with NCEP 2.5^o reanalysis data, and integrated for 60 h.

2. Mesoscale Environment and Rainfall Distribution

From the 45-km resolution simulation of the MM5 model, a baroclinic cyclone with minimum pressure of 990 hPa at surface, which originated from the Atlantic Ocean, approached Spain at 10/20/00Z. At the same time, a surface high-pressure system was located in northern Europe with a maximum pressure of 1032 hPa. The low-pressure system deepened slightly to 988 hPa at 10/20/12Z, which kept moving toward east. During this time period, the surface easterly flow, which was associated with the high-pressure system in northern Europe, split into two branches at the eastern tip of the major west-east oriented Alpine ridge. The southern branch of this easterly flow was able to penetrate to the southern foothills of the Alps and the Lago Maggiore Target Area (LMTA). At 10/21/06Z, just before the maximum rainfall occurred, the flow over the Adriatic Sea became more southeasterly (Fig. 1a). The numerical simulation was able to reproduce the major features of the surface flow. The easterly flow also turned to southeasterly. This southeasterly flow over the Adriatic Sea was blocked by the Alps and deflected to become easterly barrier jet, as also observed by Bouquet and Smull (2003) and simulated by Rotunno and Ferretti (2003). At 850 hPa, the flow to the south of the Alps was dominated by the southeasterly or southerly flow (Fig. 1b), which was able to ride over the surface cold, stable easterly barrier jet. At 300 hPa, a long and wide jet stream had meandered from the Atlantic coast of western Europe to Black Sea. At 10/21/00Z, a diffluence region was located over the Po Valley and Ligurian Sea (Fig. 1c), which appeared to provide lifting and helped enhance the low-level upward motionr. Compared to IOP-2B, the upper-level baroclinic wave was located further to the south of the Alps, which may help produce upward motion and convection further to the south.

Figure 2 shows the sounding observed at Gagliari at 10/21/06Z. Surprisingly, the CAPE at this time reached quite a high value of 2304 Jkg^{-1}, which is comparable to the CAPE observed in IOP-2B at 9/19/23Z (2000 Jkg^{-1}) at the same location (Stein 2002). Figure 3 shows the observed and model simulated 6h accumulated rainfall ending at 10/21/12Z. The numerically simulated rainfall was able to catch the basic rainfall pattern, which shows two maximum rainfall regions, the smaller over the southern Alpine slopes and the larger over the Ligurian Apennines. One deficiency of the model prediction is that the predicted rainfall over the Po Valley is much weaker than that observed. A sensitivity test with a larger domain of 5-km resolution initiated directly from the 45-km resolution domain produced a second rainfall maximum over the Po Valley, more in line with observations. Figure 3b also shows a mesoscale vortex with the diameter comparable

to that of Po Valley formed in between the Ligurian Apennines and the Lago Maggiore area. In fact, there was a LLJ flowing out to the sea in between the Ligurian Apennines and the French Alps, which is consistent with observation (Bousquet and Smull 2003; their Fig. 7a). This southward flow from the barrier jet helped produce heavy rainfall over the Ligurian Apennines. Another sensitivity test without the presence of the Ligurian Apennines indicates that the maximum rainfall was located over the Po Valley, instead of over the Ligurian Apennines.

Figure 4a shows the θ_e and vector wind fields and cloud areas on a south-north section across 10^oE at 10/21/06Z. There was a convectively unstable layer of air over the Ligurian Sea. Some shallow convective clouds have developed over the Ligurian Apennines. A cold dome, however, formed over the southern Alpine slope and extended to far upstream covering the whole Po Valley blocked the southerly and southeasterly flow. The vector wind field indicates that the flow was either very weak or even reversed in the cold dome, while the flow from the Ligurian Sea was forced to go over the cold dome and then formed shallow cloud. The cold dome acted as an obstacle to the incoming flow. In other words, the *effective mountain* is composed by both the real mountain and the cold dome, which then has a gentler slope than the real mountain. The immediate effect of the reduction of effective mountain steepness is to reduce the vertical velocity forced by the mountain, which is roughly proportional to $U\frac{\partial h}{\partial x}$. This might also contribute to the lighter rainfall, even though the air over the ocean was conditionally unstable (Fig. 2). Figure 4b shows the same cross section as in Fig. 4a, but for the potential vorticity field. Unlike that in IOP-2B, the higher-level PV and lower-level PV were not coupled in this case, which may also help explain the lighter rainfall over the southern Alpine slopes. Figures 4c and 4d show a W-E vertical section across 45^oN. Figure. 4c indicates that the easterly barrier jet is cold, stable, and shallow. The wind then turned to westerly above this cold and stable layer. Similar to the S-N cross section, the clouds are stable and shallow. The lower-level PV was mainly associated with the cloud region and above the cold and stable layer, but not coypled with higher-level PV. (Fig. 4d)

Acknowledgments: This work is supported by the US NSF Grant ATM-0096876. The computing was performed on the supercomputers at the North Carolina Supercomputer Center.

References

Bousquet, O., and B. F. Smull, 2003: Observations and impacts of upstream blocking during a widespread orographic precipitation event. Quart. J. Roy. Meteor. Soc., 129, 391-410.

Houze, R., S. Medina, and M. Steiner, 2000: Two cases of heavy rain on the Mediterranean side of the Alps in MAP. Preprints, 9th Conf. on Mountain Meteorology, 1-5, Amer. Meteor. Soc., Aspen, CO.7-11 August.

Lin, Y.-L., S. Chiao, J. A. Thurman, T.-A. Wang, M. L. Kaplan, and R. P. Weglarz, 2001: Some common ingredients for heavy orographic rainfall and their potential application for prediction. Weather and Forecasting, 16, 633-660.

Rotunno, R., and R. Ferretti, 2003: Orographic effects on rainfall in MAP IOP2B and IOP8. Quart. J. Roy. Meteor. Soc., 129, 373-390.

Stein, J., 2002: Moist airflow regimes over more or less smooth mountains. 178-181. 10th Conf. on Mountain Meteor., 17-21 June, Park City, Utah.

(a) surface 1999/10/21/06Z

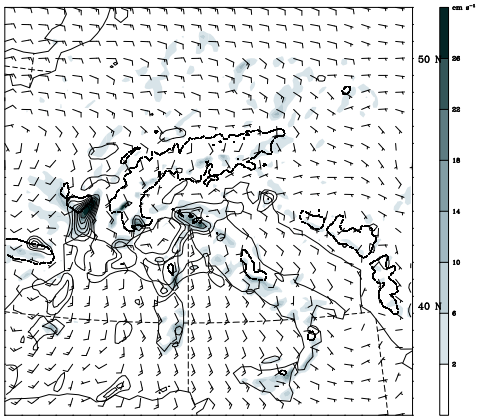

(b) 850 hPa 1999/10/21/06Z

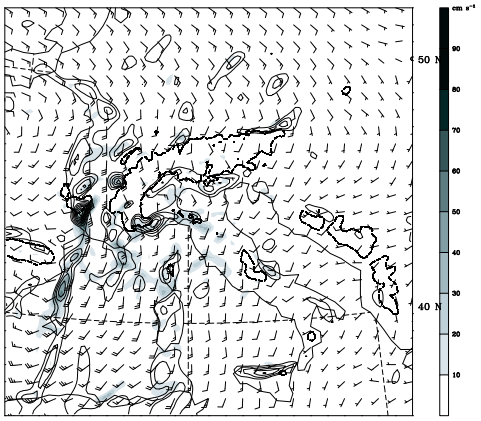

(c) 300 hPa 1999/10/21/06Z

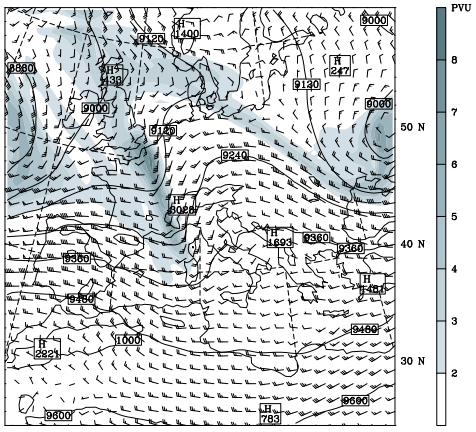

Figure 1: (a) Wind vectors and upward motion at surface for 10/21/06Z, (b) Same as (a) except at 850 hPa, and (c) Wind vectors and PV at 300 hPa for 10/21/06Z.

Sounding 1999/10/21/06Z

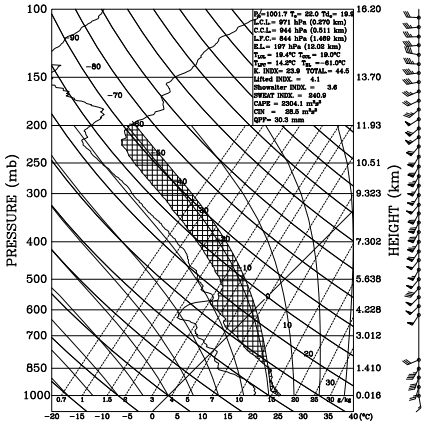

Figure 2: Sounding observed at Gagliari (southern tip of Sardinia) at 10/21/06Z. The CAPE was 2304 Jkg^{-1}.

(a) Observed rainfall 1999/10/21/12Z

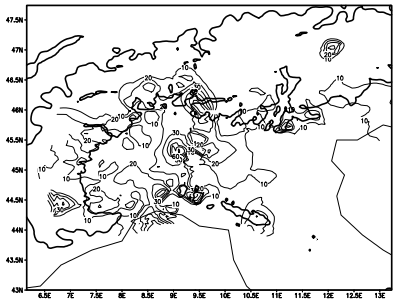

(b) Simulated rainfall 1999/10/21/12Z

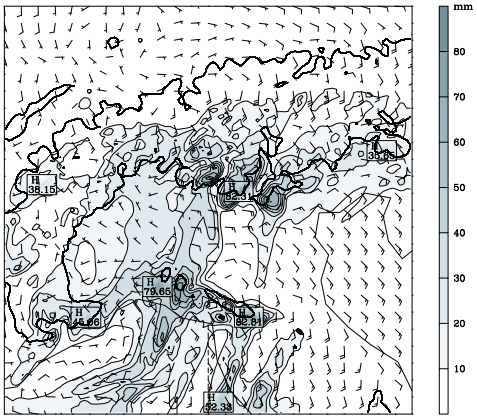

Figure 3: Observed (a) and simulated (b) 6h accumulated rainfall (in mm) ending at 10/21/12Z.

(a) S-N Cross-Section 10/21/06Z

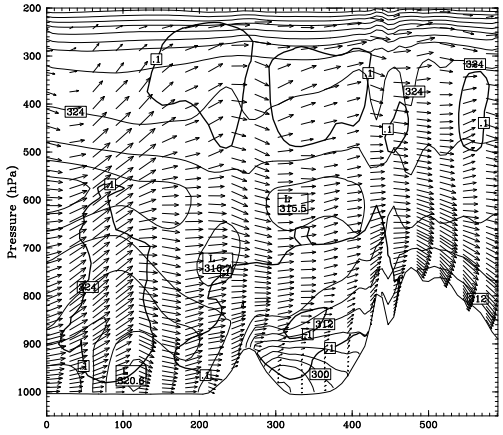

(b) S-N Cross-Section 10/21/06Z

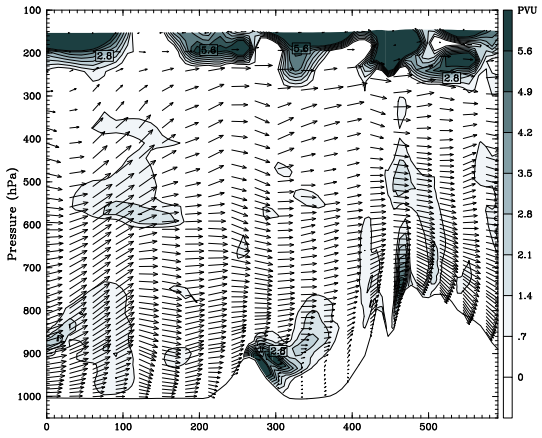

(c) W-E Cross-Section 10/21/06Z

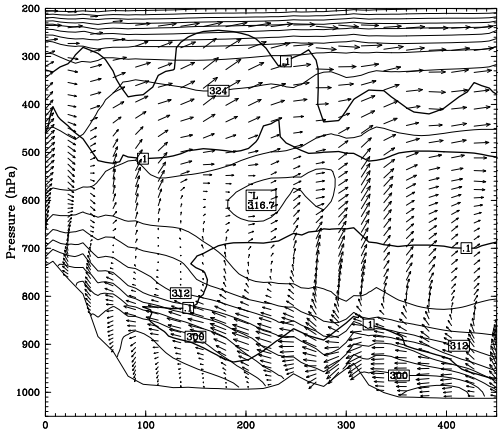

(d) W-E Cross-Section 10/21/06Z

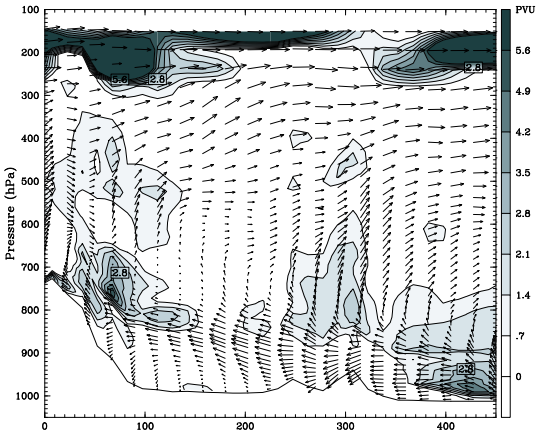

Figure 4: (a) S-N cross section at 10^oE at 10/21/12Z for θ_e, wind vectors, and cloud boundaries; (b) Same as (a) except for PV; (c) Same as (a) except for W-E cross section at 45^oN; and (d) Same as (d) except for PV.